

CONSTRAINT CONDITIONAL FINITE ELEMENT MODEL OF INTERFACIAL DEBONDING WITH ANISOTROPIC FRICTION

T. Yamaguchi^{1*}, K. Goda² and R. Kitamura³

¹ Graduate School of Science and Engineering, Yamaguchi University, Ube, Japan

² Department of Mechanical Engineering, Yamaguchi University, Ube, Japan

³ Department of Mechanical Engineering, Tokyo University of Science, Chiba, Japan

*v055ve@yamaguchi-u.ac.jp

Keywords: CMC (Ceramic Matrix Composites), Matrix crack, Interfacial debonding, FEM (Finite Element Method)

ABSTRACT

Ceramic matrix composites (CMCs), such as SiC fiber-reinforced SiC, are a damage tolerance material in which high toughness is achieved through damage mechanism such as fiber bridging, fiber pullout, interfacial debonding followed by sliding, crack deflection. The purpose of this study is to extend the constrained conditional finite element method (CC-FEM) formulated in previous studies to the case of interfacial debonding problem with anisotropic friction. The accuracy of the CC-FEM was investigated by comparing with the general purpose FEM software (ANSYS). As a result, it was found that the friction force perpendicular to the loading direction did not occur clearly in ANSYS when an uniaxial compressive load was applied. On the other hand, it occurred in the analysis of CC-FEM. In general, the friction force in the actual phenomenon must work in the perpendicular direction because it extends in the transverse direction through Poisson's effect. Therefore, it was estimated that the proposed CC-FEM gave a more accurate analysis.

1. Introduction

Ceramics are excellent in heat, abrasion and corrosion resistances, but the toughness and strength reliability are not enough due to their brittle nature. On the other hand, fiber-reinforced ceramic matrix composites (CMCs), such as SiC fiber-reinforced SiC, are a damage tolerance material in which high toughness is achieved through damage mechanism such as fiber bridging, fiber pullout, interfacial debonding followed by sliding, crack deflection [1]. From such an excellent property, CMCs are expected as a high-temperature structural material used in the field of aerospace in which conventional metals are difficult to be applied.

In general, contact problems are solvable through computational algorithms such as penalty method and enlarged Lagrange method, which are installed in the software for finite element method (FEM). In these algorithms, the computation is repeatedly carried out until the amounts of sliding and/or overlapping between nodal-points reach to a given allowable value. Therefore, the computation time and precision depend on the value [2]. On the other hand, the constrained conditional finite element method (CC-FEM) is a mechanical model, in which the equivalence of nodal-point displacements and

the equilibrium of contact forces are given as contact conditions, i.e. constrained conditions, on the contact face. According to this model, the exact numerical solution is obtainable by just one time computation without any repetition. If this model is applied to the damage problem in CMCs, even complicated damage state including plural matrix cracks and fiber breaks could be solved by only one time without divergence. In the previous papers, we formulated CC-FEM in the cases of on- and off-axial interfacial debonding problems [1, 3-5].

The purpose of this study is to extend the CC-FEM to the case of two-dimensional interfacial debonding problem. After interfacial debonding, the fiber and matrix slide each other, and stop at the mechanically balanced state, at which the frictional resistances are not necessarily identical in any sliding direction on the contact face. In this case, the problem has to be formulated by considering the anisotropic friction [6]. The present paper shows the analysis method of CC-FEM of this case and compare it with general-purpose finite element analysis software ANSYS.

2. Finite element model and method

2.1 Stiffness equation including contact forces

Once a fiber is broken or matrix crack occurs, interfacial debonding occurs in a CMC material, and then the whole stiffness of the material is reduced, resulting in a non-linear behavior in the stress-strain relation. For the analysis of this phenomenon, updated K matrix including damages such as fiber breaks and matrix cracks is incorporated into the conventional analysis [1]. In this situation, the principle of virtual work including contact forces is given, as follows:

$$\iiint_V \sigma_{ij} \delta \varepsilon_{ij} dV - \left(\iiint_V \bar{p}_i \delta u_i dV + \iint_{S_\sigma} \bar{T}_i \delta u_i dS \right) - \iint_C \Delta \bar{R}_i \delta u_i dS = 0 \quad (1)$$

where σ_{ij} , ε_{ij} , \bar{p}_i and u_i are components of stress, strain, body force and displacement in an elastic body, respectively. \bar{T}_i and \bar{R}_i are surface and contact forces, respectively. C is a contact surface and S_σ is a mechanical boundary except C . The subscripts i and j correspond to x -, y - or z -direction, and δ represents the amount of variation. By discretizing Eq. (1) and defining the equivalent nodal force on nodes of each element, the stiffness equation element $\{\Delta Q\}$ can be derived as an incremental form, as shown in Eq. (2)

$$[K]\{\Delta u\} = \{\Delta f\} + \{\Delta Q\} \quad (2)$$

where $[K]$ is the global stiffness matrix derived from the first term of Eq. (1), $\{\Delta u\}$ is the nodal displacement increment, $\{\Delta f\}$ is the load increment deriving from 2nd terms of Eq. (1), and $\{\Delta Q\}$ is the contact force increment and treated as an unknown variable vector.

2.2. Definition of interfacial contact states and conditions

CC-FEM has applied for the model of axial symmetry [1, 3-5]. In this study, we develop a new model in order to extend it to three-dimensional version. We assume interfacial contact states as (a) bonding and (b) interfacial debonding. In the latter state, (b) interfacial debonding, the concept of

anisotropic friction is applied in order to increase the versatility of CC-FEM, in which the constrained conditions are given assuming that the friction coefficients in the x and y -directions are different.

Figure 1 shows the schematic of such states, where double-nodes were assigned at the identical coordinate. Node 1 belongs to the fiber element, and node 2 belongs to the matrix one. These interfacial contact conditions are given as Eqs. (3)-(4):

(a) Bonding

When the interface is bonded without debonding as in Fig. 1(a), the continuities of displacement and the force balances are given as:

$$\begin{aligned} \Delta u_1 &= \Delta u_2, \Delta v_1 = \Delta v_2, \Delta w_1 = \Delta w_2 \\ \Delta R_{x1} + \Delta R_{x2} &= 0, \Delta R_{y1} + \Delta R_{y2} = 0, \Delta R_{z1} + \Delta R_{z2} = 0 \end{aligned} \quad (3)$$

Where, Δu , Δv and Δw are displacement increments along x , y and z -directions. ΔR_x , ΔR_y and ΔR_z are contact force increments along x , y and z -directions of nodes 1 and 2.

(b) Interfacial debonding

When the interface is debonded, and slid along x and y -directions as in Fig. 1(b), the continuities of displacement and the force balances are given as:

$$\begin{aligned} \Delta w_1 &= \Delta w_2 \\ (\Delta R_{x1} + \Delta R_{x2}) &= 0, (\Delta R_{y1} + \Delta R_{y2}) = 0, (\Delta R_{z1} + \Delta R_{z2}) = 0 \\ \Delta R_{z1} &= \sqrt{\left(\frac{\Delta R_{x1}}{\mu_x}\right)^2 + \left(\frac{\Delta R_{y1}}{\mu_y}\right)^2}, \Delta R_{y1} = \alpha \Delta R_{x1} \end{aligned} \quad (4)$$

Where, μ_x and μ_y are the coefficients of static friction in x - and y -directions, respectively. α is the relative ratio of ΔR_x and ΔR_y , and it is unknown at each double-nodes of the interface. In this study, ‘appropriate α ’ in each double-node was treated as a problem of optimization. That is to say, the ‘appropriate α ’ was decided by maximizing the frictional work W_f given as Eq. (5), based on the principle of maximum dissipation energy.

$$W_f = \sum_{i=1}^n \left(\sqrt{\Delta R_{xi}^2 + \Delta R_{yi}^2} \times \sqrt{\Delta u_{xi}^2 + \Delta u_{yi}^2} \right) \quad (5)$$

Where, n is the number of double-nodes. Each α is renewed using the genetic algorithm [7]. First, $W_f^{(1)}$ is calculated by randomly assigned α . Similarly, next α is calculated from the average of each α of the largest W_f and the second largest W_f . Thus, the ‘appropriate α ’ is found repeatedly with alternation of generations.

2.3. Insertion of the interfacial contact conditions into the stiffness equation

By inserting the interfacial contact conditions of Eqs. (3), (4) into the stiffness equation (Eq. (2)), the interfacial contact stiffness equation is given as:

$$[K_c]\{\Delta u_c\} = \{\Delta f\} \quad (6)$$

Where, $[K_c]$ is the partly changed stiffness matrix by interfacial contact conditions, of which the detail is shown in the reference [1, 3-5], and $\{\Delta u_c\}$ is the nodal displacement vector which contains nodal contact force (e.g. ΔR_x , ΔR_y and ΔR_z). From Eq. (6), $\{\Delta u_c\}$ can be calculated by the Gaussian elimination, and the nodal displacement $\{\Delta u\}$ can be obtained by the continuities of displacement as in Eqs. (3), (4).

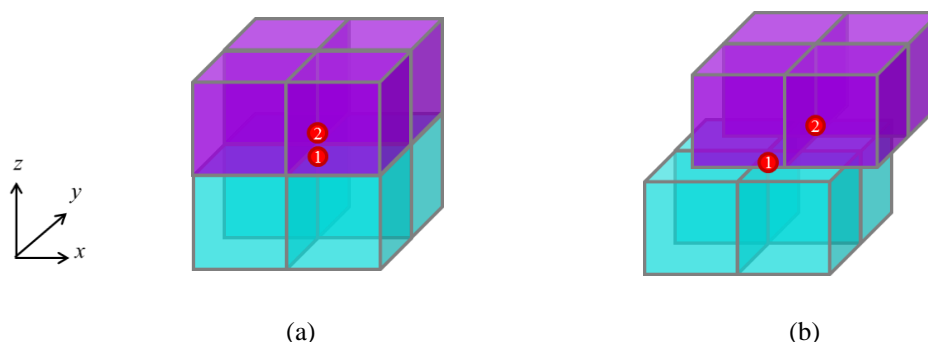


Figure 1. Interfacial contact states (a) Bonding, (b) Interfacial shear debonding

2.4. Element and boundary conditions

Shape of the final model should be assumed here as a cylindrical shape, but, in order to confirm the validity of three-dimensional CC-FEM, the interface was assumed as a plane. Figure 2 shows a model of the geometry and boundary conditions. Assuming that the final model is a cylindrical shape, the boundary conditions were defined as shown in Table 1.

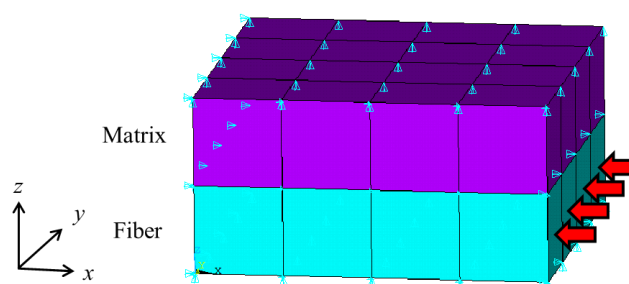


Figure 2. Finite element model

Table 1. Boundary conditions

Fixed in the x -direction	Surface of $x = 0$
Fixed in the y -direction	Surface of $y = 0$
Fixed in the z -direction	Surface of $z = 0$ or $z = z_{max}$
Displacement in the x -direction	Surface of $x = x_{max}$ and Fiber side

3. Simulation results of CC-FEM and comparison with general-purpose finite element analysis ANSYS

The results from CC-FEM and general-purpose finite element analysis software ANSYS are shown in Figs.3 and 4 (where, RV is the reference value). The present simulation treats the case that, all double-nodes at interface are debonding. The material constants used are as follows: Young's modulus $E_f = E_m = 200$ GPa, Poisson's ratio $\nu_f = \nu_m = 0.2$ and the coefficient of static friction of x and y -directions $\mu_x = \mu_y = 0.5$.

From Figs. 3 and 4, it was found that the both displacement vectors of the fiber side are very similar, whereas the vectors of the matrix side show different behavior. The reason why ANSYS's displacements in the y -direction is smaller than CC-FEM's may be suspected such that ANSYS does not consider the frictional coefficient of the vertical direction to the loading direction in the case of single-axial load. Therefore, the contact condition shown in Eq. (4) was changed as Eq. (7).

(b)' Interfacial debonding 2

$$\begin{aligned} \Delta w_1 &= \Delta w_2 \\ (\Delta R_{x1} + \Delta R_{x2}) &= 0, (\Delta R_{y1} + \Delta R_{y2}) = 0, (\Delta R_{z1} + \Delta R_{z2}) = 0 \\ \Delta R_{x1} &= \mu_x \Delta R_{z1}, \Delta R_{y1} = \mu_y \Delta R_{z1} \end{aligned} \quad (7)$$

In this calculation, μ_x and μ_y were assumed as $\mu_x = 0.5$, $\mu_y = 0$. The model used was the same as shown in the above. The results are shown in Fig.5. The comparison between Figs. 3 and 5 shows a good agreement each other. Therefore, it is estimated that the friction coefficient in the direction perpendicular to the loading direction is not considered in ANSYS. In the actual phenomenon, however, the friction force has to work in y -direction because it extends in the transverse direction though Poisson's effect. Therefore, it is estimated that the CC-FEM gives more accurate analysis. To verify the present results, as a future work, we intend to carry out the experiment of this phenomenon and compare the both results.

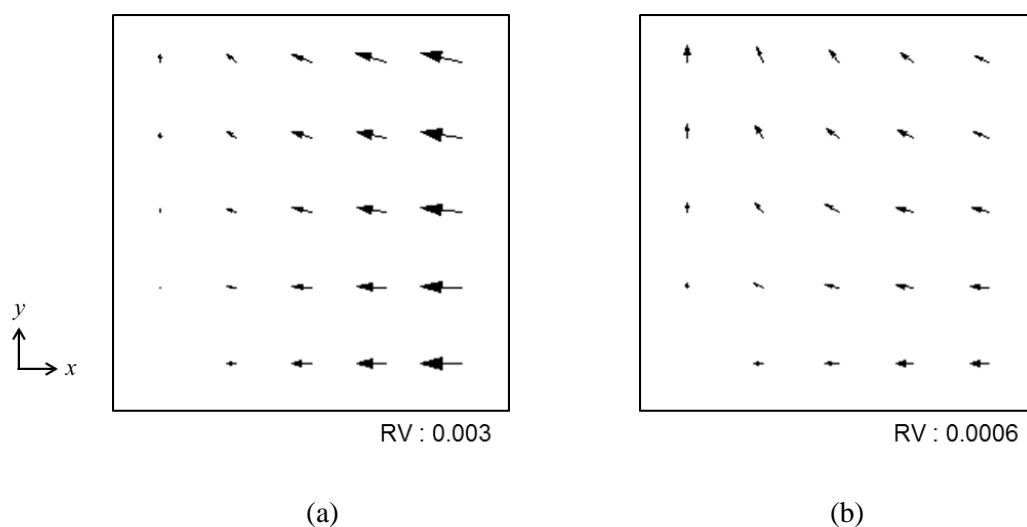


Figure 3. Displacement vectors at the interface by general-purpose finite element analysis software ANSYS. (a) fiber side, (b) matrix side.

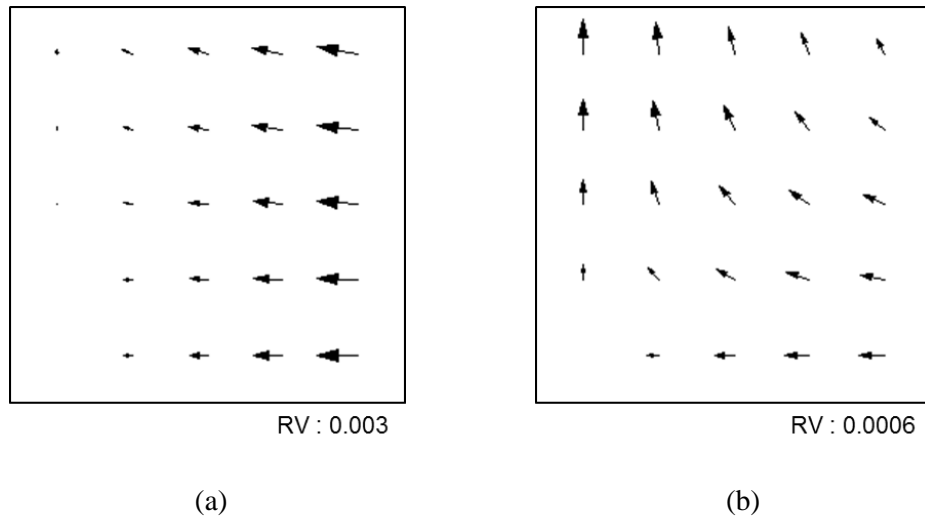


Figure 4. Displacement vectors at the interface by CC-FEM. (a) fiber side, (b) matrix side.

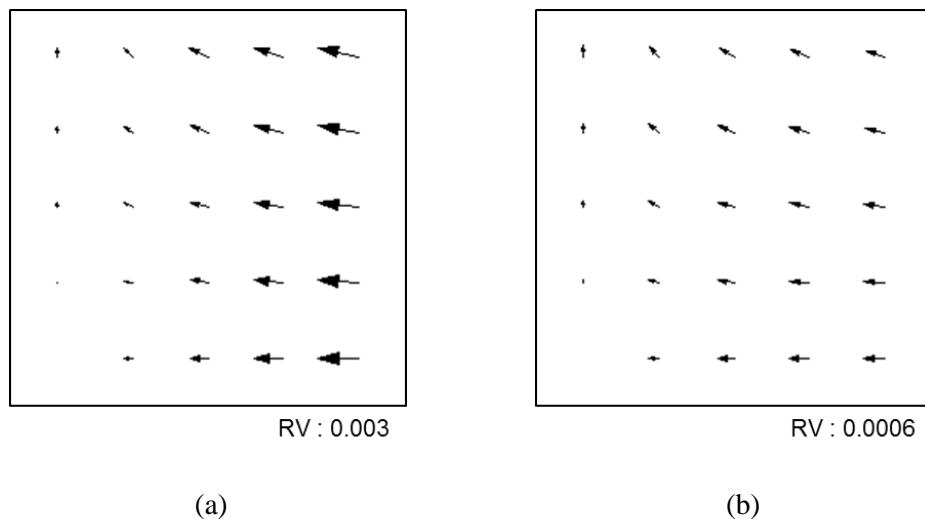


Figure 5. Displacement vectors at the interface by CC-FEM taking into account Eq. (7). (a) fiber side, (b) matrix side.

4. Conclusion

In this study, we defined a new constrained conditional finite element method (CC-FEM) in order to extend two-dimensional model to three-dimensional version. We assumed interfacial contact states as (a) bonding and (b) interfacial debonding. In the latter state, anisotropic friction and genetic algorithm were introduced. The accuracy of this model was validated in comparison with the result of the general-purpose finite element analysis software ANSYS. ANSYS's results showed that the matrix movement due to the friction force was smaller. In particular, the y-direction of the movement is too small. This is attributed to that ANSYS does not consider the vertical direction of the friction coefficient in the loading direction in the case of single-axis load. The friction force has in the actual phenomenon has to work in y- direction because of Poisson's effect. Therefore, it was estimated that the CC-FEM gives more accurate analysis.

References

- [1] K. Goda *et al.* FEM Formulation and Strength Simulation by Interfacial Contact Model of Fiber-Reinforced Ceramic Matrix Composites, *Journal of the Japan Society for Composite Materials*, Volme31:184-191, 2005.
- [2] P. H. Geubelle, J. S. Baylor, Impact-induced delamination of composites: a 2D simulation, *Composites: Part B*, 29, 589-603, 1998.
- [3] R. Kitamura, K. Goda, Verification of damage model of ceramic matrix composites and analysis of cyclic deformation behavior, *Transactions of the Japan Society of Mechanical Engineers*, 80, SMM0080, 2014.
- [4] R. Kitamura, K. Goda, Application of Conditional Finite Element Model to Ceramics Matrix Composites with Interfacial Debonding, *Journal of the Adhesion Society of Japan*, 50, 428-434, 2014.
- [5] R. Kitamura, et al. Finite Element Model for Interfacial debonding simulation of a Fiber-Reinforced Ceramic Matrix Composite, *Journal of the Japan Society for Composite Materials*, 41, 106-111, 2015.
- [6] H. Cho and J. R. Barber, Stability of the three-dimensional Coulomb friction law, *Proc. R. Soc. Lond. A* 455, 839-861, 1999.
- [7] A. Klarbring, Contact, friction, discrete mechanical structures and mathematical programming: New Developments in Contact Problems, P. Wriggers and P. Panagiotopoulos (eds.), Springer-Verlag, pp. 55–100, 1999.